Structure and Morphology of Isotactic Polypropylene Functionalized by Electron Beam Irradiation

RONG GUAN

Polymer Research Institute, Chengdu University of Science and Technology, Chengdu 610065, China

Received 23 April 1999; accepted 3 August 1999

ABSTRACT: The structure and morphology of isotactic polypropylene (iPP), functionalized by electron beam irradiation at room temperature in air, are investigated by elementary analysis, FT-infrared (FTIR) spectroscopy, electron spectroscopy for chemical analysis (ESCA), polariscope, and static contact angle. Elementary analysis reveals that the element oxygen has been introduced onto iPP chains after electron beam irradiation. In addition, as shown from FTIR spectra, oxygen-containing groups, such as carbonyl, carboxyl, and ether groups, are introduced onto iPP molecular chains. The dependence of oxygenation extent (as measured by O_{1S}/C_{1S} value of ESCA spectra) on electron beam dose is obtained. Under polariscope, it can be observed that the dominant alpha phase appears to become more enhanced, and there is no crystalline phase transition. The static contact angle of iPP decreases with increasing dose. © 2000 John Wiley & Sons, Inc. J Appl Polym Sci 76: 75–82, 2000

Key words: isotactic polypropylene; structure; morphology; electron beam; irradiation

INTRODUCTION

The major characteristic necessary for blending isotactic polypropylene (iPP) with inorganic fillers and other engineering plastics is the compatibility between components. Better compatibility can be obtained through reactive blending of functionalized iPP with other components. Usually the way to functionalize iPP is to graft polar monomers onto iPP molecular chains,[1–6] such as grafting maleic anhydride,[7] acrylic acid,[8] and acrylates,[9] by melting, solution, solid, and gas grafting techniques. These grafting techniques, however, are complex, overelaborate in posttreatment, and some of them even pollute the environment and damage the apparatus. Furthermore, to carry out the grafting, monomers and other auxiliaries must be added, which would then bring the negative effects on the thermal, electrical, and hygienic properties of blends, caused by the residue and homopolymer of the added monomers. Recently, Xu[10] used γ-ray, electron beam, ultraviolet, and microwave irradiation techniques to functionalize polyethylene (PE) without adding any monomers and auxiliaries in air, significantly enhancing the compatibility of PE with the inorganic fillers and other engineering plastics, and obtained stronger and tougher PE materials.

In this study, we examine the changes in structure of iPP samples irradiated by electron beam at room temperature in air. The variations in oxygen content were analyzed by elementary analysis. FTIR and ESCA were used to characterize the oxygen-containing groups of iPP after electron beam irradiation. The polariscope was used to observe the iPP spherulitic morphology. The static contact angle study revealed that irradi-

Correspondence to: R. Guan, Faculty of Chemistry and Materials, Hubei University, Wuhan, 430062, China (rongguan@public.wh.hb.cn).

Journal of Applied Polymer Science, Vol. 76, 75–82 (2000)

Table I Elemental Analysis Data for Electron Beam–Irradiated iPP

Sample	Dose (kGy)	O (%)	C (%)	H (%)	N (%)
EBP1	0.0	0.56	86.64	13.19	0
EBP2	0.5	0.99	86.46	13.06	0
EBP3	0.75	1.30	86.26	12.93	0
EBP4	1.0	1.50	86.62	12.67	0
EBP5	5.0	1.86	86.00	12.68	0

ated iPP exhibits higher hydrophilicity than nonirradiated iPP.

EXPERIMENTAL

Materials and Sample Preparation

Commercial samples of iPP (Yanshan Petrochemistry Company PP2401) used in this study had the following characteristics. The molecular weight (M_w) was 2.40×10^5, the melt index 2.5 g/10 min, and the density ranged from 900 to 910 kg/m^3. Material was obtained from a commercial iPP manufacturer in China.

Films of 50–200 μm thickness were obtained by pressing the material in a hydraulic press maintained at 192 ± 2°C. The samples were allowed to remain in the press for about 8 min, after which the samples were pressed under another cold hydraulic press at room temperature for 5 min. The films for polariscope analysis were prepared by melting the polymer in the press at 192°C, then isothermally crystallizing at 130°C for 1 h.

Electron Beam Irradiation

The samples were kept in an aluminum tray and placed under the source window. The source of radiation was a static electricity accelerator; the set dose was obtained through adjusting the energy and beam current. The samples were irradiated in a lower dose range (0–5 kGy) and a higher dose range (0–100 kGy), respectively, at room temperature in air.

Elementary Analysis

Elementary analysis was carried out on a CARLOERBA 1106 analyzer to analyze the percentage content of carbon, hydrogen, oxygen, and nitrogen.

FTIR Spectroscopy

FTIR analysis was performed using a Nicolet 560 series FT-infrared spectrometer. The films were scanned from 4000 to 400 cm^{-1} with a resolution of 4 cm^{-1}, scanning number 26. Relevant portions of the spectra depicting the change in the carbonyl and hydroxyl content have been compared.

Electron Spectroscopy for Chemical Analysis

ESCA spectra were recorded on a KRATON XSAM 800 Spectrometer with AlKα source ($h\nu$

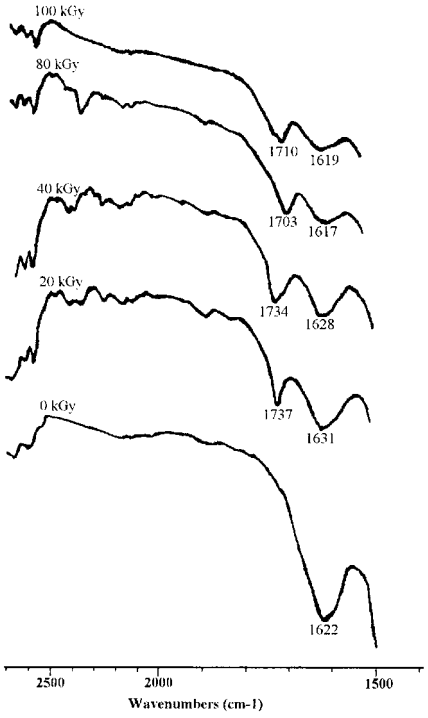

Figure 1 FTIR spectra of electron beam–irradiated iPP (energy, 1.75 MeV; beam current, 30 μA).

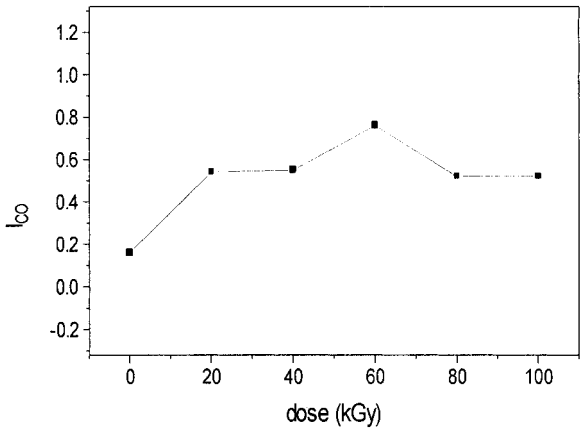

Figure 2 The rate of formation of carbonyl versus higher dose (energy, 1.75 MeV; beam current, 30 μA).

= 1486.6 eV, 0.83 nm). The C_{1S} peaks were fitting resolved according to Gauss distribution in a computer.

Polariscope Observation

Polariscope observations were carried out on the isothermally crystallized iPP samples at room temperature, using LEITZ polariscope equipped with a ×400 camera lens.

Static Contact Angle

Static contact angle testing of iPP samples with distilled water was carried out on Ermag-I instrument at 10°C.

RESULTS AND DISCUSSION

Elementary Analysis

A change in the oxygen content of the electron beam–irradiated samples is evident in the elementary analysis data of Table I. Relative to the nonirradiated iPP, each of the irradiated iPP samples caused an obvious increase in oxygen content. Specifically, it is important to note that the oxygen content of iPP increases from 0.56 to 1.86% with increasing electron beam dose under the experimental conditions examined. According to the data presented in Table I, there is no introduction of nitrogen during the electron beam irradiation process.

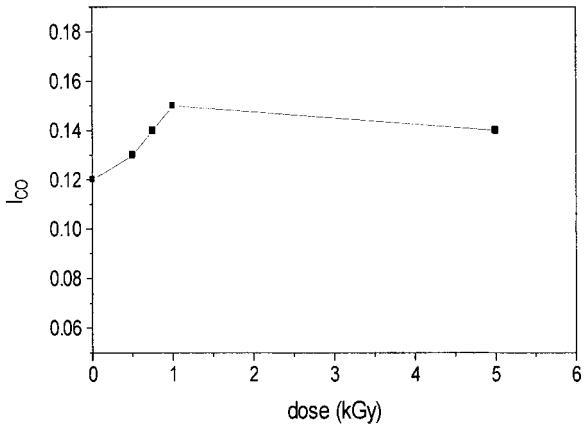

Figure 3 The rate of formation of carbonyl versus lower dose (energy, 1.75 MeV; beam current, 5 μA).

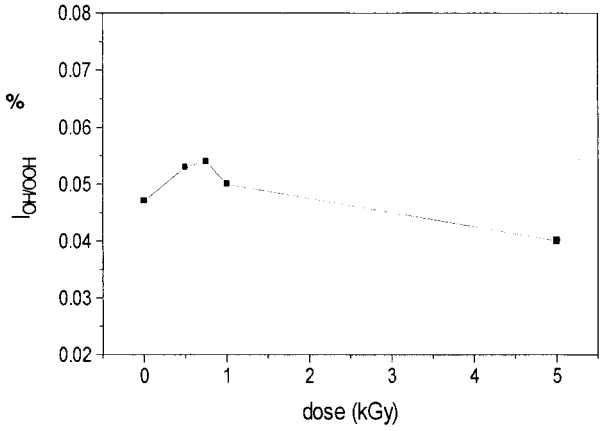

Figure 4 The rate of formation of hydroxyl versus dose.

FTIR Spectroscopy

Figure 1 shows FTIR traces of iPP irradiated at higher electron beam dose range. It is apparent

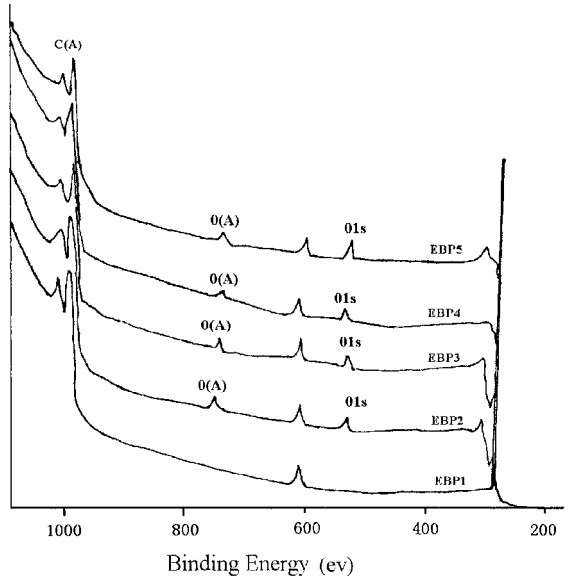

Figure 5 Wide scanning ESCA spectrum for electron beam–irradiated iPP. (a) Electron beam doses: (a) 0 kGy; (b) 0.5 kGy; (c) 1.0 kGy; (d) 5.0 kGy.

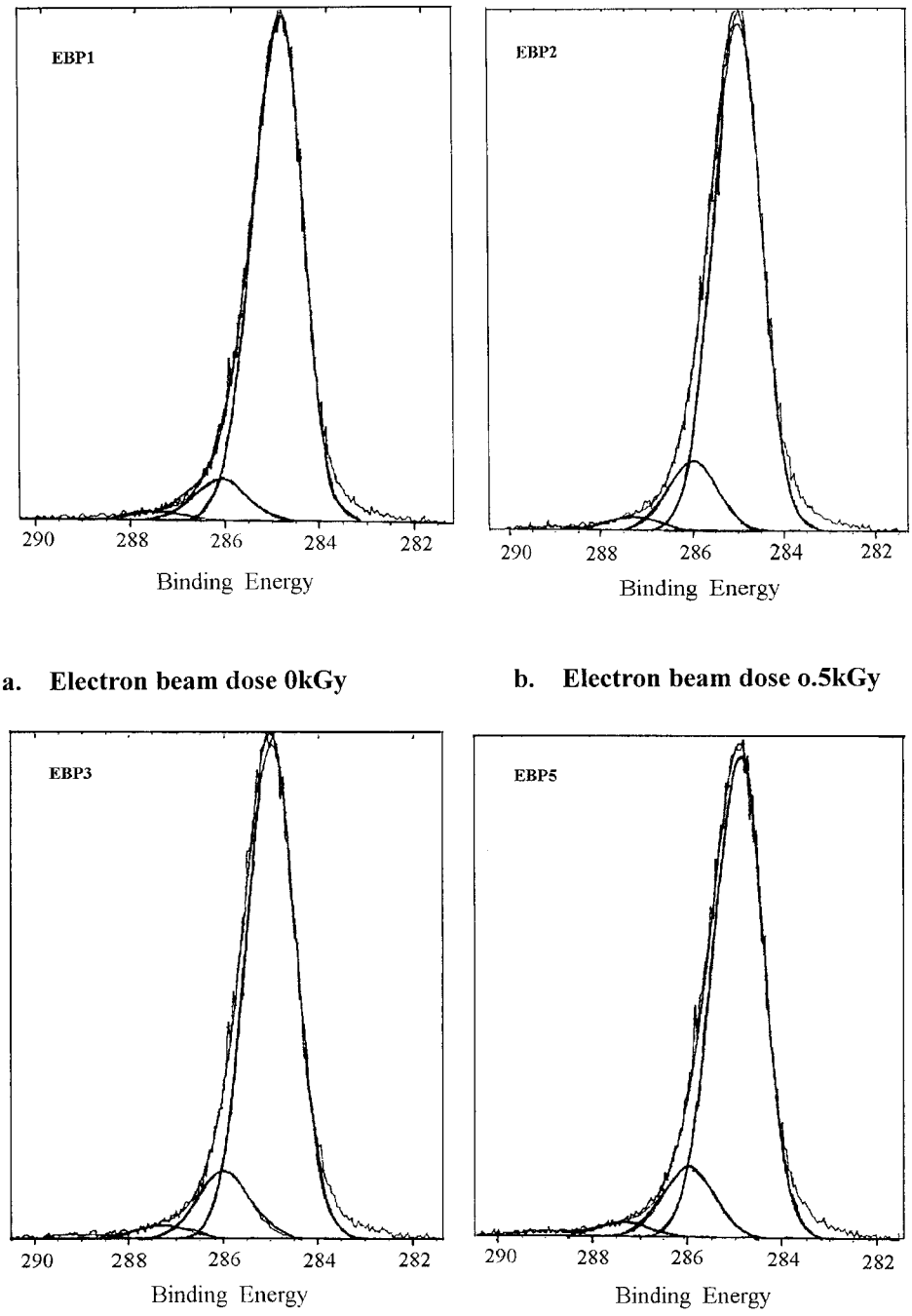

a. Electron beam dose 0kGy **b. Electron beam dose o.5kGy**

c. Electron beam dose 1kGy **d. Electron beam dose 5kGy**

Figure 6 The C_{1S} spectra of electron beam–irradiated iPP.

that, after irradiation, a new absorption peak appears around 1710 cm^{-1} in FTIR spectra, indicating that the oxygen-containing groups such as carbonyl, carboxylic, and ether have been introduced onto iPP molecular chains. Because the frequency of the carbonyl group stretching vibration is dependent on various factors, different structure environments of the C═O group will cause the shift of the frequency,[11] and the more electronegative an atom or group di-

Table II The C_{1S} and O_{1S} Data for Electron Beam–Irradiated iPP

	C_{1S}			O_{1S}		
Sample	Binding Energy (eV)	Width (eV)	Atomic Conc. (%)	Binding Energy (eV)	Width (eV)	Atomic Conc. (%)
EBP1	285.0	1.23	99.24	532.8	0.05	0.76
EBP2	285.1	1.29	98.35	532.5	0.65	1.65
EBP3	284.9	1.29	98.35	533.3	0.14	1.65
EBP4	285.1	1.35	98.51	532.5	0.19	1.49
EBP5	285.0	1.30	98.33	533.3	0.37	1.67

rectly attached to a carbonyl group, the greater the frequency. The carbonyl frequency can thus be assigned as —CC(═O)C— (1717 cm^{-1}), —CC(═O)OH (1712 cm^{-1}), and —C(═O)OC— (1748–1730 cm^{-1}), respectively.

To know the introduction rate of oxygen-containing groups onto iPP chains (the rate of oxidation), it is usual to monitor the hydroxyl (OH/OOH) group formation ($I_{OH/OOH}$) at 3450–3400 cm^{-1} and/or carbonyl (CO) group formation (I_{CO}) at 1720–1700 cm^{-1} using the following expressions, respectively[11]:

$$I_{OH/OOH} = \frac{\text{Absorbance at 3450–3400 cm}^{-1}}{\text{Absorbance of reference peak}} \quad (1)$$

$$I_{CO} = \frac{\text{Absorbance at 1720–1710 cm}^{-1}}{\text{Absorbance of reference peak}} \quad (2)$$

Absorbance of a reference peak compensates for changes in film thickness and should not change with oxidation time; here we select absorption around 900 cm^{-1} as the reference peak. The effects of electron beam dose on the hydroxyl and carbonyl group formation are shown in Figures 2–4. In higher dose and lower dose scope (the difference is in dose rate—the former has a higher dose rate, the latter a lower dose rate), the formation of the hydroxyl and carbonyl groups initially increases, followed by a decrease with increasing electron beam dose. Since oxidation products increase with decreasing dose rate,[13] the higher the dose rate, the less oxidation will be evident; however, in order to get the good FTIR spectrum to avoid the disturbance peak from the antioxidants, the higher dose irradiation was carried out by using the iPP that contained no antioxidants, which led to an increase of oxidation products. Therefore, the amount of carbonyl content in higher dose irradiation in Figure 2 is larger than that in lower dose irradiation in Figure 3. And with dose increases, the oxidation under the surface layer of iPP will decrease due to the slower

Table III The C_{1S} of ESCA Analysis Data for Electron Beam–Irradiated iPP

	Sample EB Dose	EBP1 (0 kGy)	EBP 2 (0.5 kGy)	EBP3 (0.75 kGy)	EBP4 (1 kGy)	EBP5 (5 kGy)
$\underline{C}H_2$	Binding energy (eV)	285.0	285.0	285.0	285.0	285.0
	FWHM (eV)	1.3	1.3	1.3	1.3	1.3
	Area (%)	87.7	82.6	82.5	82.7	82.2
$\underline{C}$—O	Binding energy (eV)	286.1	286.0	286.0	286.0	286.0
	FWHM (eV)	1.3	1.3	1.3	1.3	1.3
	Area (%)	7.2	11.2	11.3	10.8	11.7
$\underline{C}$═O	Binding energy (eV)	287.4	287.3	287.3	287.3	287.3
	FWHM (eV)	1.3	1.3	1.3	1.3	1.3
	Area (%)	1.3	2.1	2.1	2.0	2.3
$\underline{C}$(═O)O	Binding energy (eV)	289.1	289.0	289.0	289.0	289.0
	FWHM (eV)	1.3	1.3	1.3	1.3	1.3
	Area (%)	0.1	0.5	0.6	0.5	0.9

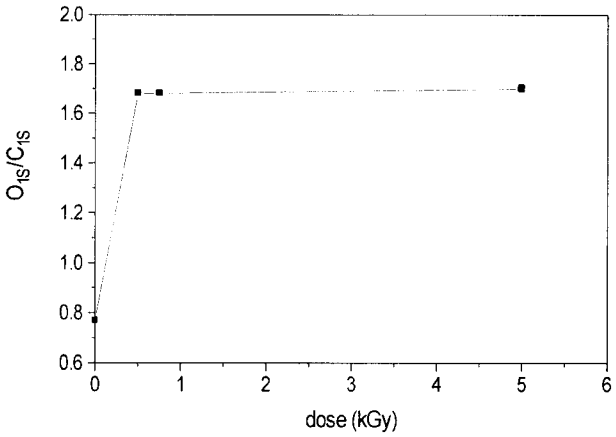

Figure 7 Change of O_{1S}/C_{1S} measured from ESCA with irradiation dose. Electron beam doses: (a) 0 kGy; (b) 0.5 kGy; (c) 0.75 kGy; (d) 1.0 kGy; (e) 5.0 kGy.

diffusion of oxygen, which accounts for decreased formation of I_{CO} and $I_{OH/OOH}$ after some dose level.

Electron Spectroscopy for Chemical Analysis

Figure 5 shows a wide scanning ESCA spectrum of iPP irradiated at lower dose scope. It is obvious that two new O_{1S} and O(A) peaks appear on the ESCA spectrum of the electron beam–irradiated iPP (samples EBP2–EBP5), meaning the oxygen incorporation into the iPP molecular chains gave rise to a variety of functional groups.

In a graphic demonstration of the oxygen incorporation, Figure 6 shows a fitting resolution of the C_{1S} peak of ESCA spectrum of iPP. Comparison of the resolved peaks of irradiated iPP (Figure 6(b)–(d) with nonirradiated iPP [Fig. 6(a)] shows that the second large C_{1S} peaks of irradiated iPP are clearly increased. Their quantitative analysis and corresponding O_{1S} peak data are listed in Table II. It can been seen that the width of C_{1S} increases from 1.23 to 1.3 eV and the atomic concentration of C_{1S} decreases from 99.24 to 98.33%, whereas the width of O_{1S} increases from 0.05 to 0.37 eV and the atomic concentration increases from 0.76 to 1.67%.

The main C_{1S} peak can be resolved into component peaks at binding energies of 285.0, 286.0, 287.4, and 289.0 eV, respectively, corresponding to carbon in $\underline{C}H_2$, $\underline{C}$—O, $\underline{C}$═O, and $\underline{C}$(═O)O. The O_{1S} peak can be decomposed into two peaks with binding energies of 532.4 and 533.8 eV, respectively. The O_{1S} peaks are assigned as follows: O_{1S} 533.8 eV (O═C—$\underline{O}$—H or O═C—$\underline{O}$—C) and O_{1S} 532.4 eV (C═$\underline{O}$ or C—$\underline{O}$).[14]

Table III reveals that after electron beam irradiation, there appeared oxygen functional groups such as carbonyl, ether, and carboxylic on the iPP surface. The main functional groups introduced are C—O and C═O. Using the ratio of O_{1S} to that of C_{1S} (O_{1S}/C_{1S}) as a measure of the surface oxygenation extent, the variation of iPP oxygenation extent can be plotted, as shown in Figure 7. At a small dose, such as 0.75 kGy, the surface of iPP is nearly completely oxidized; that is, the oxygenation on the iPP surface reaches balance rapidly. Since the ESCA analysis reflects the surface oxidation (2 nm depth of the surface) of iPP, where FTIR reveals the oxidation information down the surface 10–30 μm in depth, it is reasonable to see the difference about the variation of oxidation with dose between two analysis methods.

Polariscope Observation

Figure 8 shows five polariscope photographs of the iPP samples isothermally crystallized at 130°C. These samples contain mainly α-phase spherulites determined by WAXD,[15] and the relative content of β-phase decreases with increasing electron beam dose. On the other hand, the content of α-phase increases with increasing electron beam dose. The α-phase of iPP has a monoclinic crystal structure, with a complex crosshatched array of radial and tangential lamellar structures, and a typical radiation structure from the spherulitic center along the radial direction. From Figure 8(a)–(e), the α-spherulitic morphology becomes more and more enhanced; thus, it can be concluded that the electron beam irradiation does appear to change the structure somewhat and the dominant α-phase appears to become more enhanced.

Static Contact Angle

Figure 9 shows the variation of contact angle of iPP with distilled water at room temperature. Increasing the electron beam dose, the contact angle of irradiated iPP decreases, indicating an increase in hydrophilicity; that is, after the electron beam irradiation, iPP has higher hydrophilicity than nonirradiated iPP, so the surface hydrophilicity of iPP is improved.

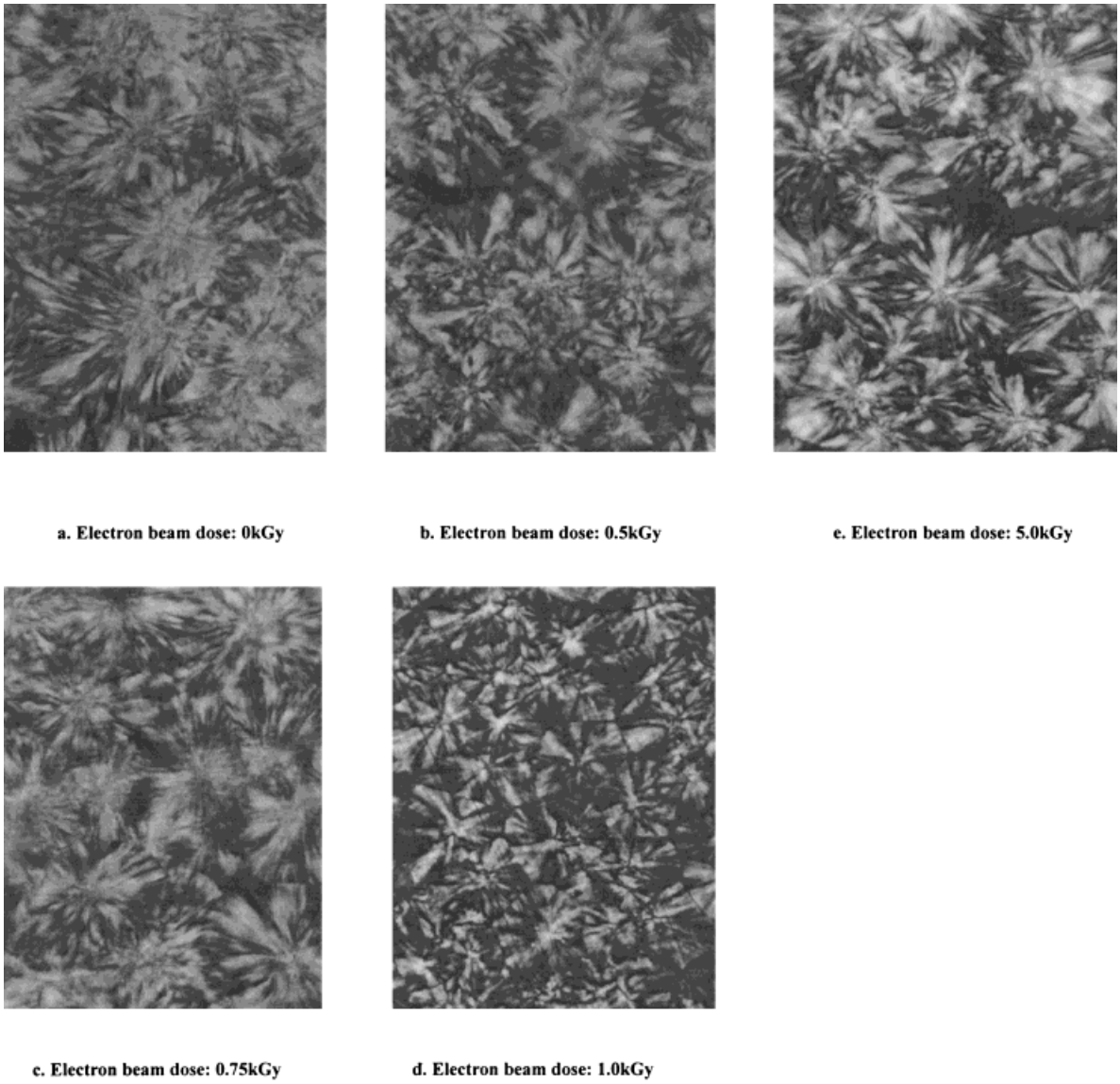

Figure 8 Polariscope photograph of electron beam–irradiated iPP (isothermal crystallization at 130°C for 1 h, ×480).

CONCLUSIONS

Isotactic polypropylene can be functionalized to contain carbonyl, carboxylic, and ether groups via an electron beam irradiation process without adding any monomers or auxiliaries in air. The irradiation dose influences the degree of surface oxidation. The atomic ratio O_{1S}/C_{1S} of ESCA spectra can be taken as a measure of the degree of surface oxidation during the electron beam irradiation process. There is no crystalline phase transition upon electron beam irradiation. The result of static contact angle measurement shows that electron beam irradiation is an effective method to improve the hydrophilicity of iPP. Furthermore, through this investigation, it can be seen that the electron beam irradiation technique to functionalize iPP offers several advantages: no chemical reagents are required and there are no residual polluting by-products or tedious posttreatment. Electron beam irradiation, therefore, is a promising technology to functionalize isotactic polypropylene in industry.

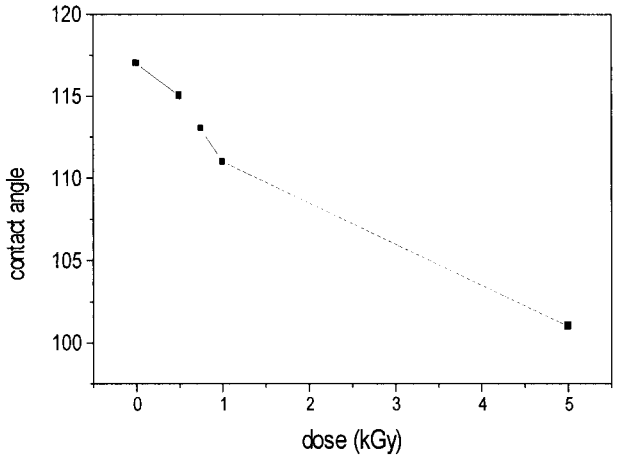

Figure 9 The contact angle of electron beam–irradiated iPP (10°C).

REFERENCES

1. Vacearo, E.; Dibenedetto, A. T.; Huang, S. J. J Appl Polym Sci 1997, 63, 275.
2. Oromehie, A. O.; Hashemi, S. A. Polym Int 1997, 42, 117.
3. Duvall, J.; Sellitti, C.; Myers, C.; Hiltner, A.; Baer, E. J Appl Polym Sci 1994, 52, 195.
4. Rengarajan, R.; Vicic, M.; Lee, S. J Appl Polym Sci 1990, 39, 1783.
5. Ho, R. M.; Su, A. C.; Hu, C. H. Polymer 1993, 34, 3264.
6. Xue, F.; Zhao, J. Q.; Huang, T.; Shen, J. R. Plast Industry 1996, 24, 58.
7. Yang, M. S. Plast Industry 1995, 23, 6.
8. Chiang, W. Y.; Yang, W. D. J Appl Polym Sci 1988, 35, 807.
9. El-Nesr, E. M. J Appl Polym Sci 1997, 63, 377.
10. Xu, X. in Proceedings of the Third China–Japan Seminar on Advanced Plastics, Polymer Alloys and Composites; Yi, X. S., Takemura, K., Eds.; Natinal Advanced Materials Committee of China: Beijing, 1998; p 1.
11. Rabek, J. F. Polymer Photodegradation; Chapman & Hall: London, 1995.
12. Carlsson, D. J.; Wiles, D. M. Macromolecules 1969, 2, 587.
13. Singh, A.; Silverman, J. Radiation Processing of Polymers; Oxford University Press: New York, 1992.
14. Bai, G. J.; Weng, Y. X.; Hu, X. Z. J Appl Polym Sci 1996, 60, 2397.
15. Guan, R. Ph.D. Thesis, Sichuan University, China, 1999.